Multiaxial Fatigue Behavior of Steels Under In-Phase and Out-of-Phase Loading Including Different Wave Forms and Frequencies

H. Dietmann T. Bhonghibhat † A. Schmid

Staatliche Materialprüfungsanstalt Universität Stuttgart
Third International Conference on Biaxial/Multiaxial Fatigue
3-6 April, 1989, Stuttgart, FRG

Abstract

In structural engineering many components are subject to cyclic loading conditions involving multiaxial—especially biaxial—stress states. In order to determine the resulting fatigue strength of the applied material under complex loading one must consider not only the various mean and alternating stress components and the number of cycles, but in addition also the time-dependance of the stress (wave form), the frequency and the phase-difference between the stress components.

This paper deals with investigations carried out on thin-walled tubular specimens out of steel St 35, loaded by cyclic internal pressure and axial forces. The objective of these investigations was to find out how the fatigue strength under in-phase and out-of-phase loading by two alternating normal stresses is influenced by the wave form of the stress vibrations (sinusoidal, triangular, trapezoidal) and by the ratio of frequency. The fatigue limits under various stress combinations as determined experimentally are then compared with theoretical results obtained by a "Modified Octahedral Shear Stress Theory" which was developed for complex fatigue loading conditions.

1 Introduction

Technical components are frequently subjected to multiaxial fatigue loading. Their endurance limit depends on the stress components as a function of time, frequency, phase difference and wave form.

In previous experiments, mainly a load combination of bending and torsion was investigated because of its practical importance [1,2]. In this case the material loading is determined by normal and shear stresses. Later on fatigue tests were carried out with a load combination of two normal stresses which were also principal stresses [3-5].

However, in certain areas of application there can occur stresses of any wave form and ratio of frequency. Therefore, the goal of the investigations presented was to determine the effect of different wave forms and frequencies of in-phase and out-of-phase alternating stresses on the fatigue limit of the materials applied. Along with the experimental investigations theoretical considerations were developed to predict fatigue failure. Based on the assumption of the existence of a critical plane, the shear stress amplitude was considered to be responsible for the material behaviour (Modified Octahedral Shear Stress Theory).

2 Experimental Tests

2.1 Material and Specimen

The multiaxial fatigue tests were carried out using tubular specimens of steel St 35 annealed (910^0C/ 45min/air) as shown in *Fig. 1.* The material data determined by tensile tests and uniaxial fatigue tests, respectively, can be seen from *Table 1.* To achieve a high quality surface, all specimens were honed at the inner surface and chemically polished at the outer surface.

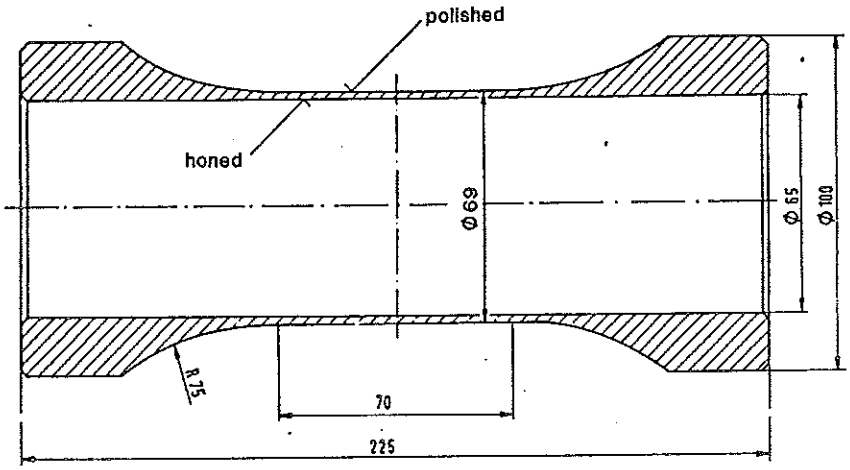

Figure 1: Thin walled tubular specimen

Static strength		
Yield stress	$R_{p0.2}$	$= 340N/mm^2$
Ultimate stress	R_m	$= 543N/mm^2$
Fatigue strength		
Alternating tension-compression	σ_W	$= 230N/mm^2$
Pulsating tension	σ_{Sch}	$= 360N/mm^2$
Alternating torsion	τ_W	$= 130N/mm^2$

Table 1: Material data of steel St 35

2.2 Test Device

The test device applied was a 2-channel servo-hydraulic testing machine as shown in *Fig. 2.* The test specimen can be loaded by longitudinal and circumferential normal stresses in-phase as well as out-of-phase, and with different wave forms. The construction of the testing device makes it possible that under internal pressure the specimens are subject only to circumferential stresses, without additional longitudinal stresses. The longitudinal stresses can be applied separately by means of a hydraulic cylinder, independent of the internal pressure. Thus the desired independence of the two normal stress components regarding wave form, frequency and phase position is assured. In order to achieve optimized load-time-functions, that is, to minimize the deviations between the nominal and real values especially in the low internal pressure range, the fatigue tests were carried out with a relatively low test frequency of maximum 1.3 Hz in relation to internal pressure.

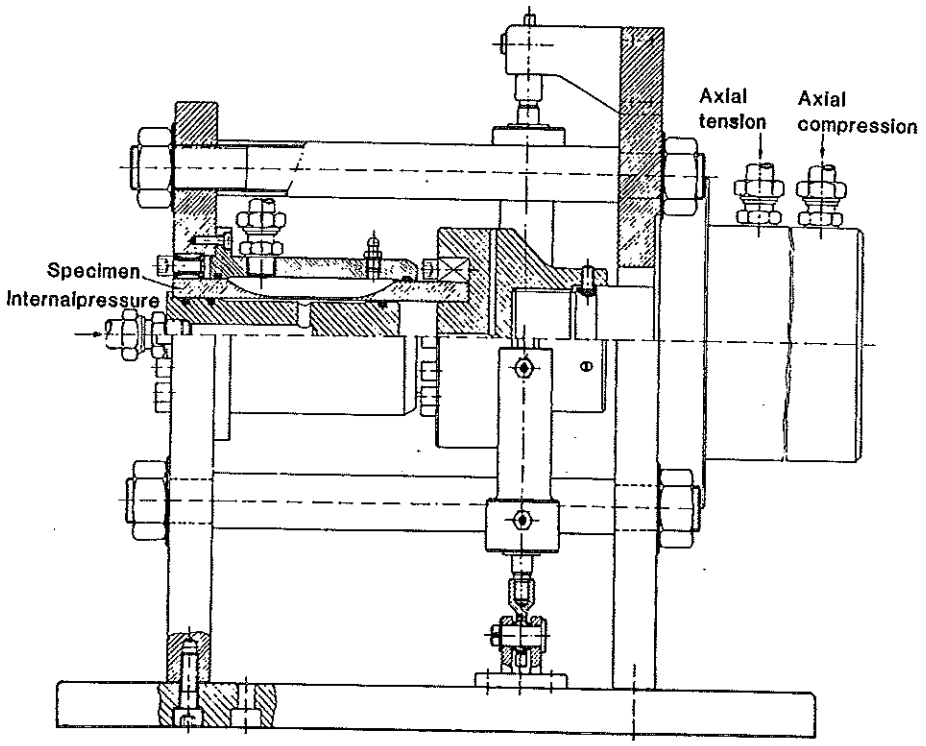

Figure 2: Test equipment for biaxial loading

2.3 Test Program

All tests for determining the influence on the wave form and different frequencies on the fatigue endurance limit were carried out under pulsating internal pressure and pulsating axial tension. In addition to the sinusoidal wave form a triangular and trapezoidal form of the load-time-function was chosen for both test series (see *Table 2*). The time of the load increase of the trapezoidal signal was 10% of the wave period. For a period of 2π this is equal to a load ascent time of $\pi/5$.

Wave form	phase difference δ	stress-time-functions
triangular	0^0 90^0 120^0 180^0	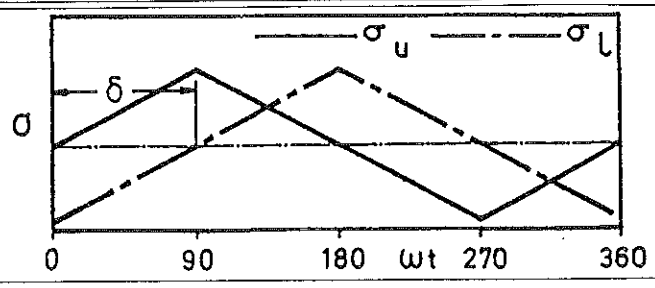
sinusoidal	(0^0) 90^0 120^0 (180^0)	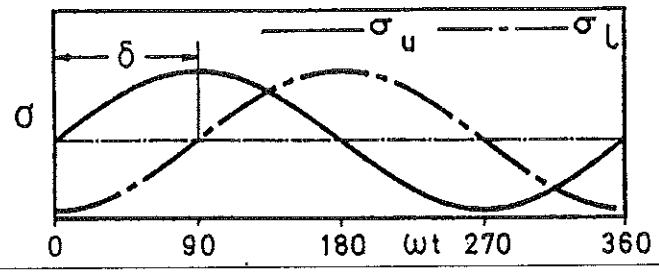
trapezoidal	(0^0) 90^0	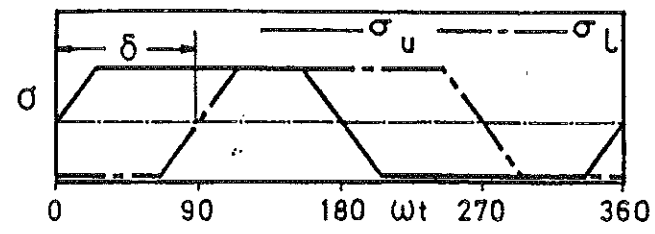
triangular	0^0 90^0	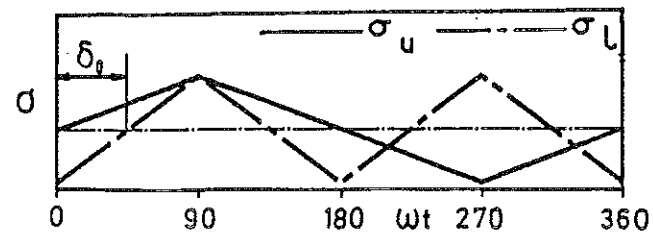
sinusoidal	0^0 90^0	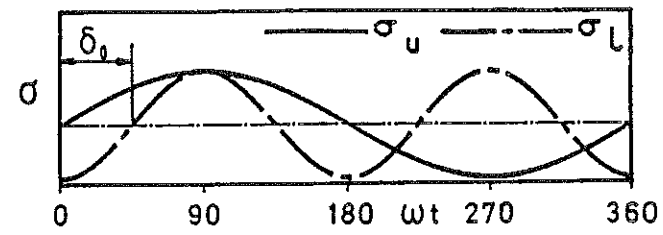
trapezoidal	0^0 90^0	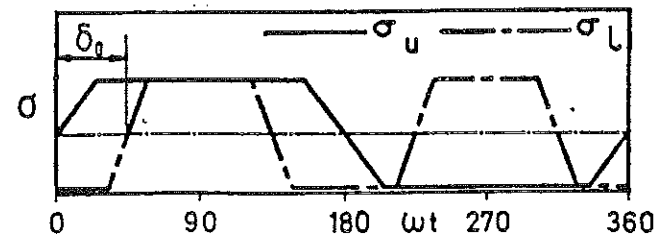

Table 2: Test program

In the test series on the influence of the wave form, the ratio of the mean stresses, amplitudes and frequencies of the two normal stresses in longitudinal and circumferential direction was kept constantly at the value 1:1. Table 2 gives a survey of the phase difference chosen hereby. The load cases with phase angles in brackets were controlled spotwise, since for synchronous loading and for a phase angle of 180^0 an influence of the wave form was not to be expected. Contrary to the test series concerning the influence of the wave form in combination with a phase-difference, in the second test series the variation of the phase angles was confined to 0^0 and 90^0. The ratio of frequencies of the longitudinal and the circumferential stresses was chosen 2:1, in relation to the longitudinal tension. The other test parameters correspond to those of the first test series.

3 Test Results

3.1 Influence of the Wave Form

The results of the experimental investigations about the influence of the wave form in combination with a phase difference on the fatigue limit of the material are shown in Figs. 3 to 7.

As from *Fig. 3* for the sinusoidal load oscillations can be seen, the fatigue strength amplitude of the circumferential stress decreases with increasing phase angle.

For time-saving reasons, the dashed Woehler curves for synchronous loading and for 180^0 phase difference were taken from the corresponding loading cases with triangular stress oscillation (see Fig. 4), since for these loading conditions theoretically no influence of the wave form should

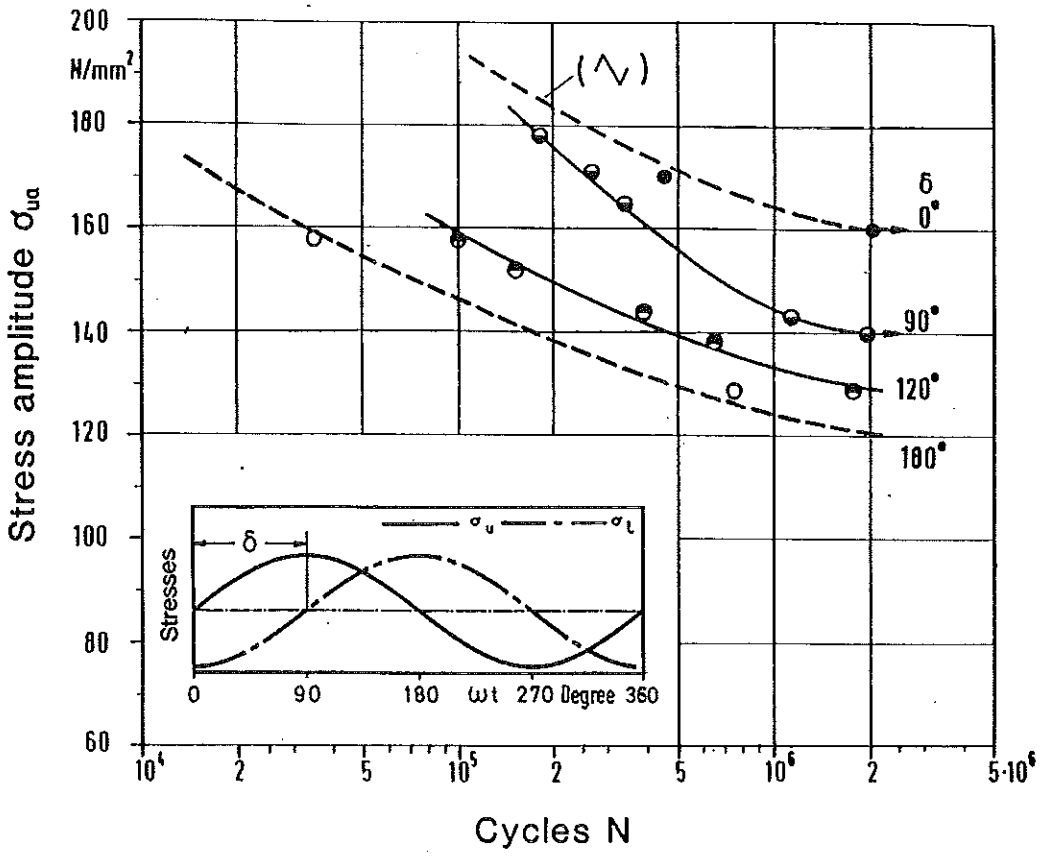

Figure 3: Test results for sinusoidal loading

occur. To ensure this assumption, for each loading case two specimens were loaded sinusoidally, and the test data were compared to the dashed Woehler curves. The good agreement between the test points and the Woehler curves justifies the assumption made above.

The fatigue strength amplitude of the circumferential stress for in- phase loading was $\sigma_{uA}(=\sigma_{lA}) = 160N/mm^2$. On the other hand, for a phase difference of 90^0 the the fatigue stress amplitude was $\sigma_{uA} = 140N/mm^2$, which means a 12.5% decrease against the in-phase loading. If the phase difference is further increased to 120^0, the fatigue stress amplitude decreases still more to $\sigma_{uA} = 129N/mm^2$. Finally, the minimum stress amplitude occurred for a phase difference of 180^0 and was $\sigma_{uA} = 120N/mm^2$, thus measuring a 25% decrease compared with in-phase conditions.

The results of the fatigue tests with triangular load oscillations are shown in *Fig. 4*. Contrary to the sinusoidal loading, the maximum fatigue stress amplitude occurred at a phase difference of 90^0 and was $\sigma_{uA} = 162N/mm^2$. This is slightly more than with the in-phase loading, where the stress amplitude $\sigma_{uA} = 160N/mm^2$ was the same as for sinusoidal oscillations. At a phase difference of 120^0 the maximum stress amplitude of $140N/mm^2$ is again higher than with sinusoidal stress amplitudes, whereas a phase difference of 180^0 yields for both wave forms the same value of $\sigma_{uA} = 120N/mm^2$.

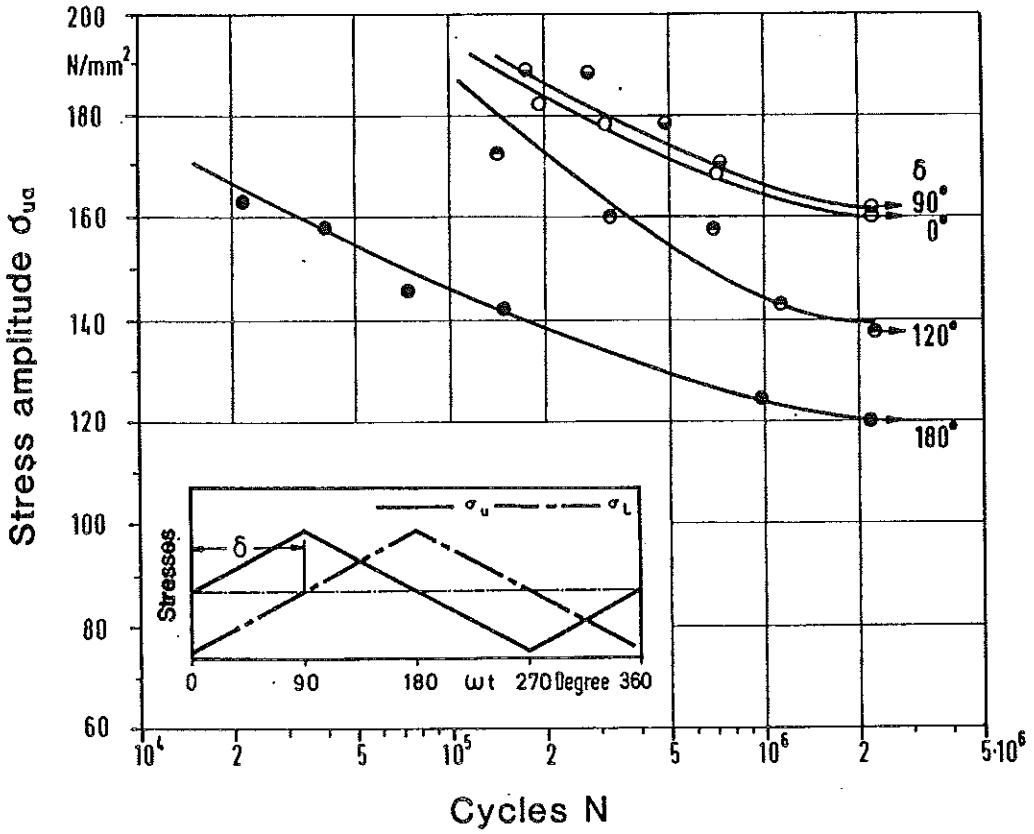

Figure 4: Test results for triangular loading

The Woehler diagram in *Fig. 5* shows the results of the fatigue tests with trapezoidal load oscillations. Again the Woehler curve for synchronous loading was taken from the corresponding Woehler diagram for triangular stress oscillations, this being controlled by two triangularly loaded specimens.

Already at a phase difference of 90^0 the maximum stress amplitude is only $\sigma_{uA} = 120 N/mm^2$, a value that occurs with sinusoidal and triangular loading only at a phase difference of 180^0. The test data of two additional specimens for 180^0 agree well with the Woehler curve for 90^0 phase difference. It can therefore be assumed that the Woehler curve for 90^0 phase difference represents also the loading with phase differences of 120^0 and 180^0.

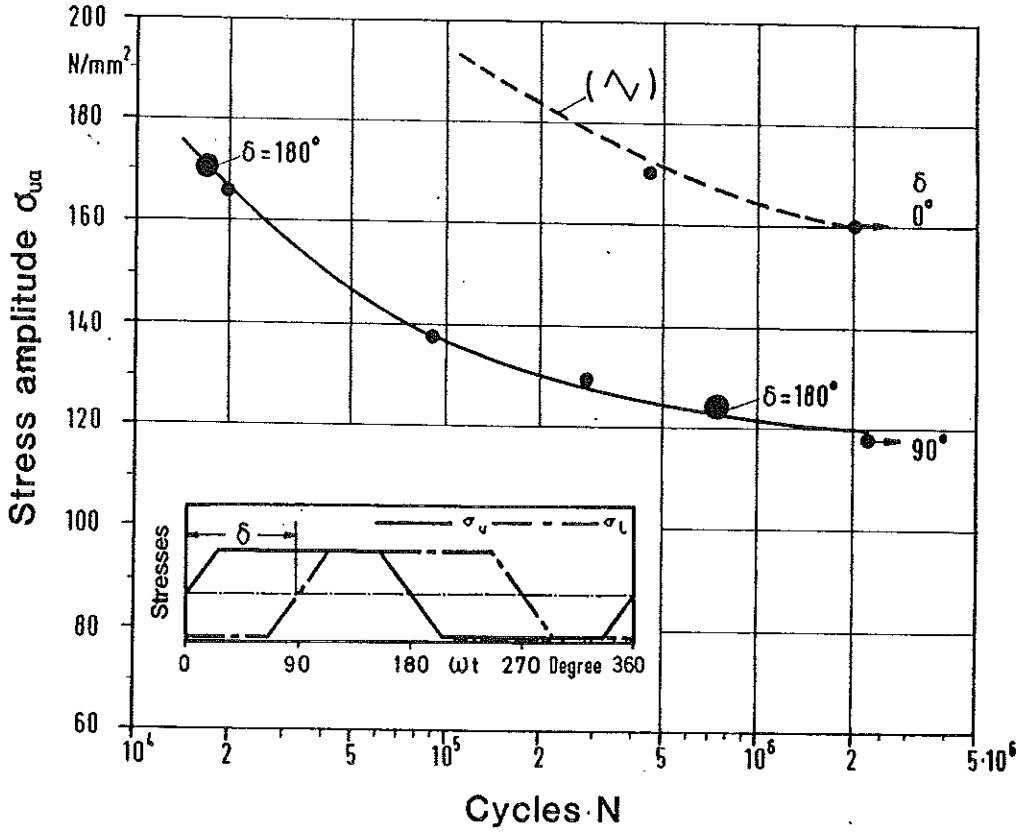

Figure 5: Test results for trapezoidal loading

Comparing the test results obtained from the three wave forms one finds the fatigue limit of the circumferential stress amplitude in all cases under synchronous biaxial loading by pulsating internal pressure and axial tension to be $\sigma_{uA} = 160 N/mm^2$. The fatigue strength of the material under uniaxial pulsating tension is $\sigma_{Sch} = 360 N/mm^2$, corresponding to a fatigue amplitude of $\sigma_{Sch}/2 = 180 N/mm^2$. The decrease of the biaxial fatigue strength compared with the uniaxial is probably due to the effect of the second mean stress in the biaxial case. The influence of the wave form in combination with a phase difference on the fatigue strength can be seen in *Figs. 6* and *7*. Here the Woehler curves for triangular, sinusoidal and trapezoidal loading and a phase difference of 90^0 and 120^0, respectively, are compared with each other. Additionally, the fatigue strength under synchronous loading is marked. The Woehler curve for trapezoidal loading in Fig. 7 was taken from Fig. 6, since due to the test results the influence of the phase difference for $\delta = 90^0$ and $\delta = 120^0$ is nearly identical. For a phase difference of 90^0 as well as for 120^0, the Woehler curves for sinusoidal loading lie in between. With regard to the material stressing, the loading conditions with triangular wave forms are the most favorable case, those with trapezoidal wave forms the least favorable one.

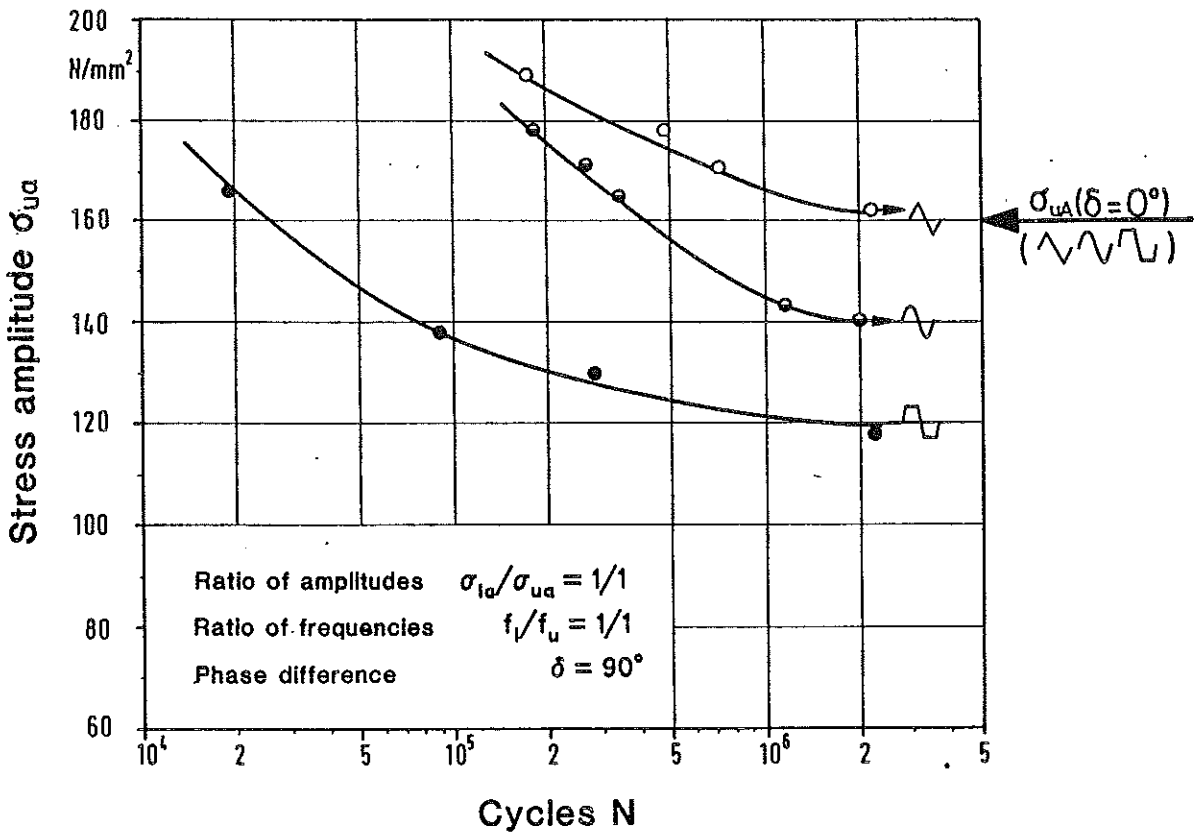

Figure 6: Influence of wave form (phase difference $\delta = 90^0$)

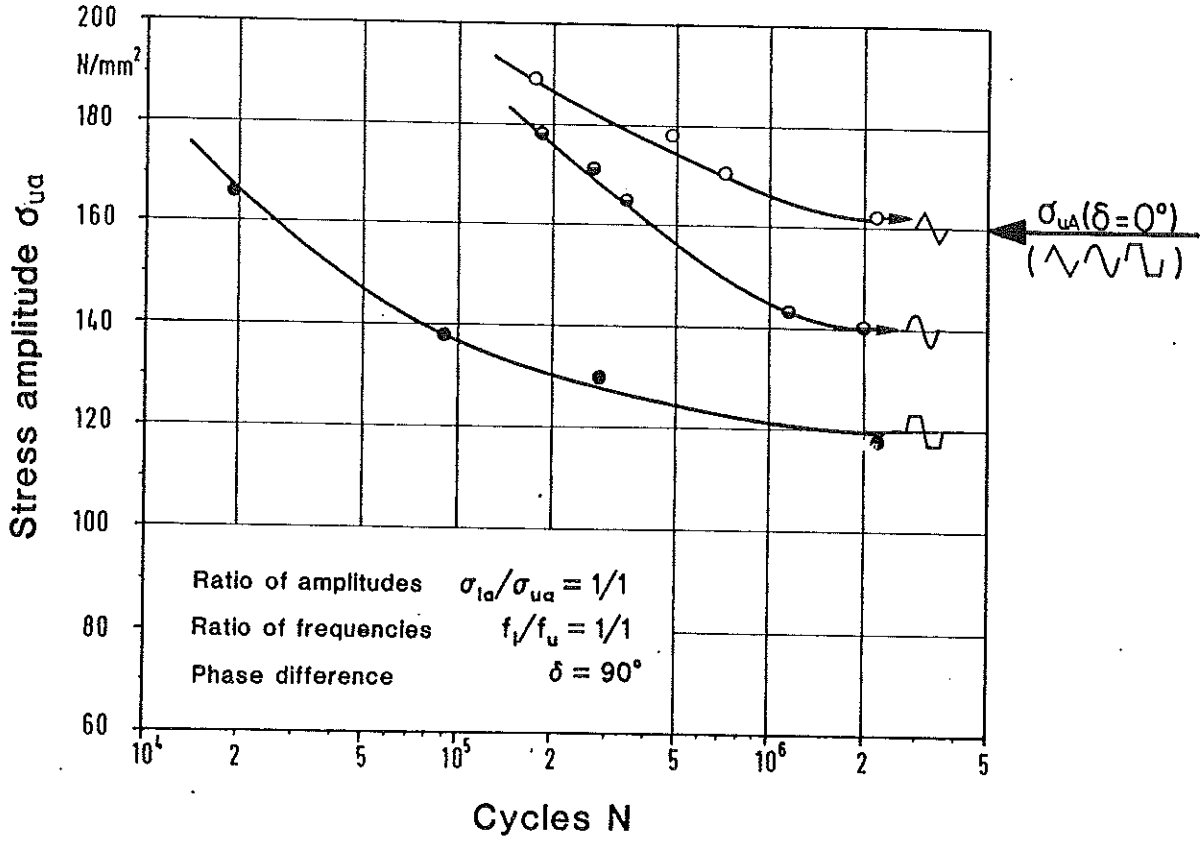

Figure 7: Influence of wave form (phase difference $\delta = 120^0$)

The ratio of the fatigue strength amplitudes σ_{uA} for out-of- phase loading and in-phase loading under triangular, sinusoidal and trapezoidal load oscillations, respectively, yields the following values:

$$\begin{aligned} \delta = 90^0: \quad & \sigma_{uA}(\delta)/\sigma_{uA}(0) = 1.01 \quad ; 0.875 \quad ; 0.75 \\ \delta = 120^0: \quad & \sigma_{uA}(\delta)/\sigma_{uA}(0) = 0.875 \quad ; 0.81 \quad ; 0.75 \end{aligned}$$

3.2 Influence of Different Frequencies

Figs. 8 to 10 show the results of the second test series, carried out under pulsating axial tension and internal pressure. The ratio of frequencies of axial tension to internal pressure was 2:1. From these test data, on the one hand the effect of different frequencies on the fatigue strength can be determined by comparing the resulting fatigue stress amplitude with initial phase difference zero to that of the corresponding synchronous case, and on the other hand, the influence of an initial phase difference can be found. For sinusoidal loading without initial phase difference ($\delta_0 = 0$) the fatigue stress amplitude amounts to $\sigma_{uA} = 131 N/mm^2$ (*Fig. 8*), as against $160 N/mm^2$ for equal frequencies. By an initial phase difference of $\delta_0 = 90^0$ the fatigue stress amplitude increases to $\sigma_{uA} = 139 N/mm^2$.

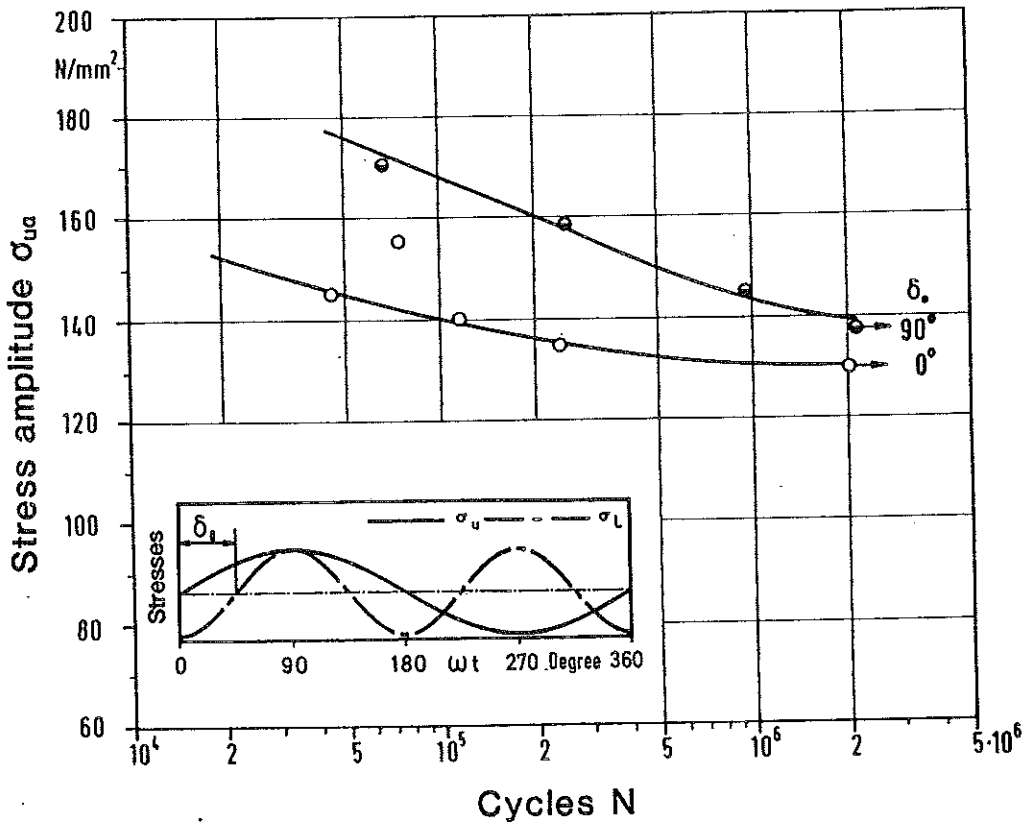

Figure 8: Test results for sinusoidal loading (frequency ratio 2:1)

In the case of triangular loading without initial phase difference the fatigue stress amplitude is $\sigma_{uA} = 144 N/mm^2$ (*Fig. 9*). By imposing an initial phase angle of $\delta_0 = 90^0$ the fatigue stress amplitude decreases slightly to $141 N/mm^2$. The strongest effect of different frequencies occurs with trapezoidal loading. Without initial phase difference the fatigue stress amplitude is $\sigma_{uA} = 119 N/mm^2$ (*Fig. 10*) (this is nearly equal to the minimum fatigue stress amplitude of $120 N/mm^2$ under equal frequencies for sinusoidal and triangular loading and a phase difference of 180^0). With an initial phase angle of $\delta_0 = 90^0$ the fatigue stress amplitude is $\sigma_{uA} = 126 N/mm^2$, which is slightly higher than without initial phase difference.

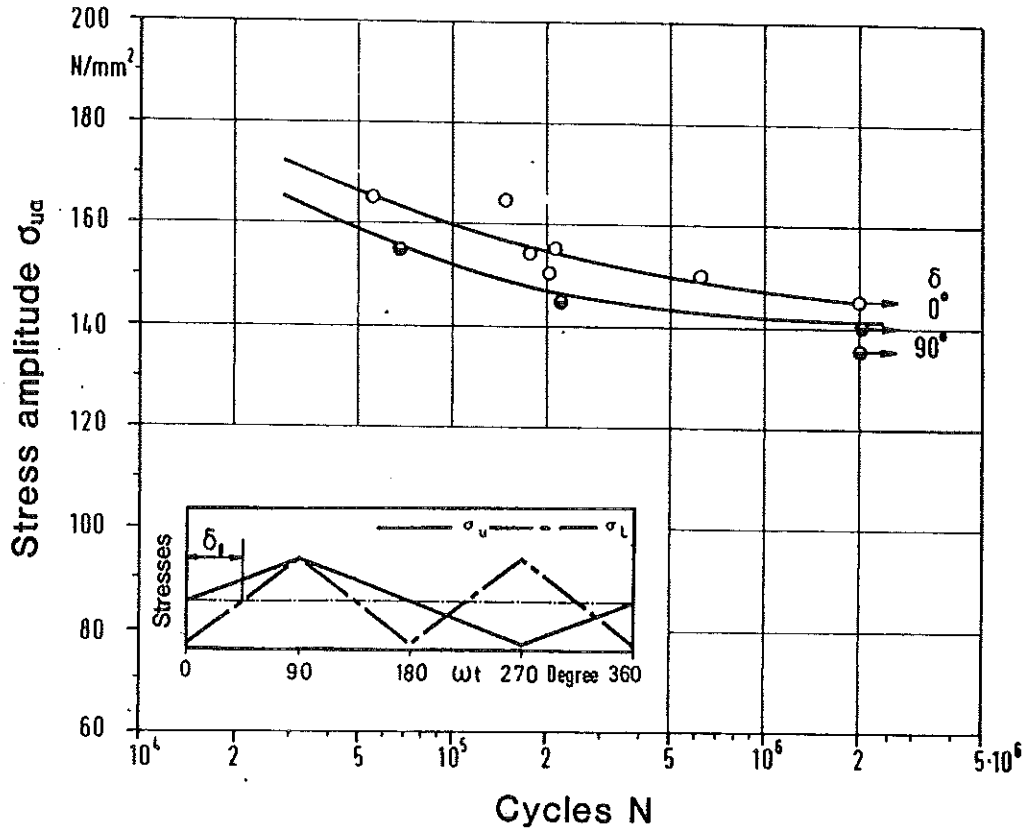

Figure 9: Test results for triangular loading (frequency ratio 2:1)

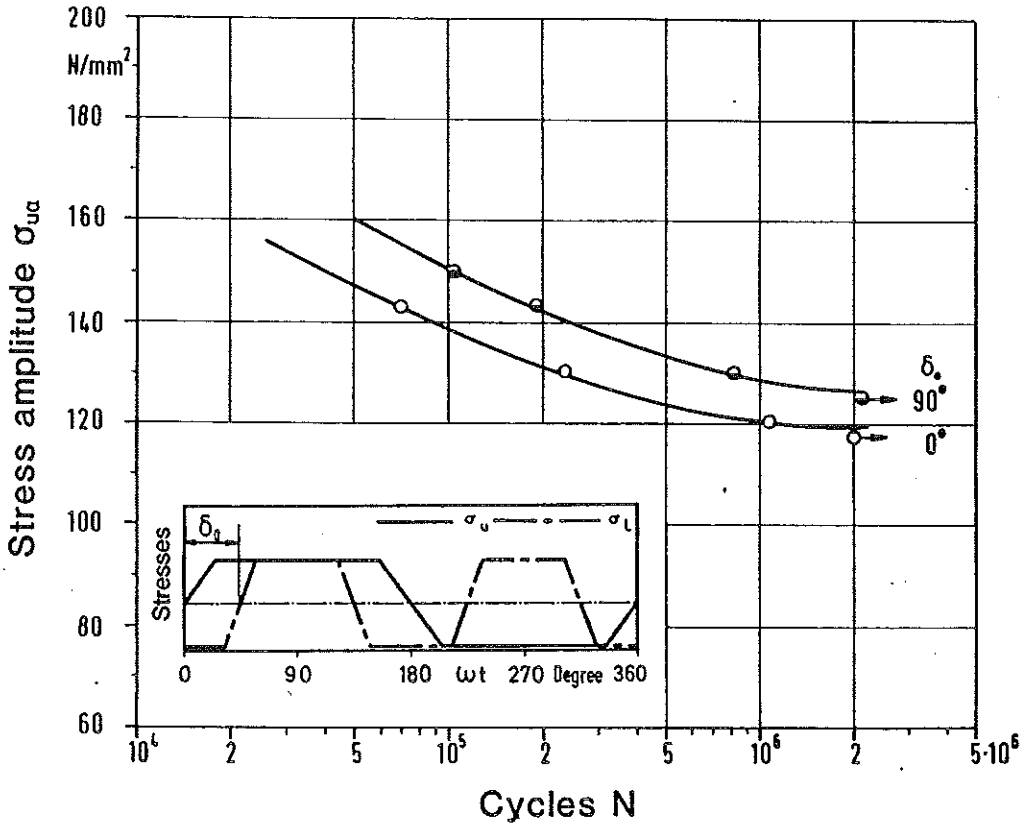

Figure 10: Test results for trapezoidal loading (frequency ratio 2:1)

It thus can be stated that in case of a frequency ratio 2:1 between longitudinal and circumferential stresses, the fatigue strength generally decreases compared to loading with equal frequencies. Again the decrease is highest for trapezoidal and lowest for triangular stress waves. An initial phase difference of $\delta_0 = 90^0$ results in a small increase of the fatigue strength for sinusoidal and trapezoidal loading, and a small decrease for triangular loading.

4 Modified Octahedral Shear Stress Theory MOSH

4.1 Basic Considerations

There are several proposals to determine the fatigue strength under complex loading conditions. In general, they are either based on the assumption of an integral material stressing expressed in energy terms, or on the existence of a critical plane where material failure occurs. Due to the integral fatigue method [6,7], the entire stress state is decisive for material failure, whereas, according to the critical plane method [8-10], only the stresses in a certain representative plane are considered responsible for failure. The Modified Octahedral Shear Stress (MOSH) theory used here, developed from the Octahedral Shear Stress Theory (OSH), is based on the latter method. While the application of the normal Octahedral Shear Stress Theory is confined to loading cases with fixed principal stress directions, the modified method can also be applied to loading conditions with rotating principal stress axes.

According to the Octahedral Shear Stress Theory the material behaviour is determined by the stresses in the octahedral plane, in particular by the amplitude of the shear stress. In multiaxial fatigue loading with constant principal stress axes, i.e. with fixed position of the octahedral plane, the fatigue stress amplitudes predicted by this theory agree well with experimental results [5]. Based on this, the theory is modified by the assumption that, also in case of rotating octahedral planes, the shear stress amplitude $\tau_{\gamma'\varphi'a}$ in the plane of the maximum oscillating octahedral shear stress ($\gamma'\varphi'$–plane) can be considered as the decisive factor determining the material behavior. *Figs. 11* and *12* show the position of the ($\gamma'\varphi'$)–plane and, as an example, the shear stress path during one complete load cycle. The shear stress amplitude determined from the stress path is then compared with the value $\tau_{\gamma'\varphi'A}$ which characterizes the material behavior in the ($\gamma'\varphi'$)–plane. This material value is derived from the fatigue limit σ_W of the material under alternating stress or the fatigue stress amplitude $\sigma_A = f(\sigma_m)$, depending on the mean stress σ_m, respectively. Material failure is then to be expected if

$$\tau_{\gamma'\varphi'a} = \tau_{\gamma'\varphi'A} \tag{1}$$

4.2 Analytical Procedure

Since the initiation of a fatigue fracture generally occurs at a load-free surface element, the calculation method is confined to biaxial stress states ($\sigma_z = \sigma_3 = 0$). In this case the octahedral plane merely rotates around the z-axis of the coordinate system (see Fig. 11). Therefore only the angle φ' has to be determined for evaluating the octahedral shear stress. The angle γ' has the constant value $\gamma' = \arccos(1/\sqrt{3})$.

The calculation of the fatigue shear stress amplitude is carried out by the following steps:

1. Determination of the ($\gamma'\varphi'$)–plane

   From the stress-time-functions the alternating stress components $\sigma_{w,x}(t)$, $\sigma_{w,y}(t)$ and $\tau_{w,xy}(t)$ can be separated to calculate the alternating octahedral shear stress $\tau_{w,oct}(t)$. The maximum value $\tau_{w,oct,max}$ and the time t_{max} at which it occurs, determine the ($\gamma'\varphi'$)–plane. Using the stresses $\sigma_x^+ = \sigma_x(t_{max})$, $\sigma_y^+ = \sigma_y(t_{max})$ and $\tau_{xy}^+ = \tau_{xy}(t_{max})$, the angle between the x-axis and the first principal stress axis at the time t_{max} is

between the x-axis and the first principal stress axis at the time t_{max} is

$$\varphi_{x1} = 0.5 \arctan \frac{-2\tau_{xy}^{+}}{\sigma_x^{+} - \sigma_y^{+}} \tag{2}$$

and thus the angle φ' is

$$\varphi' = \varphi_{x1} + 45^0$$

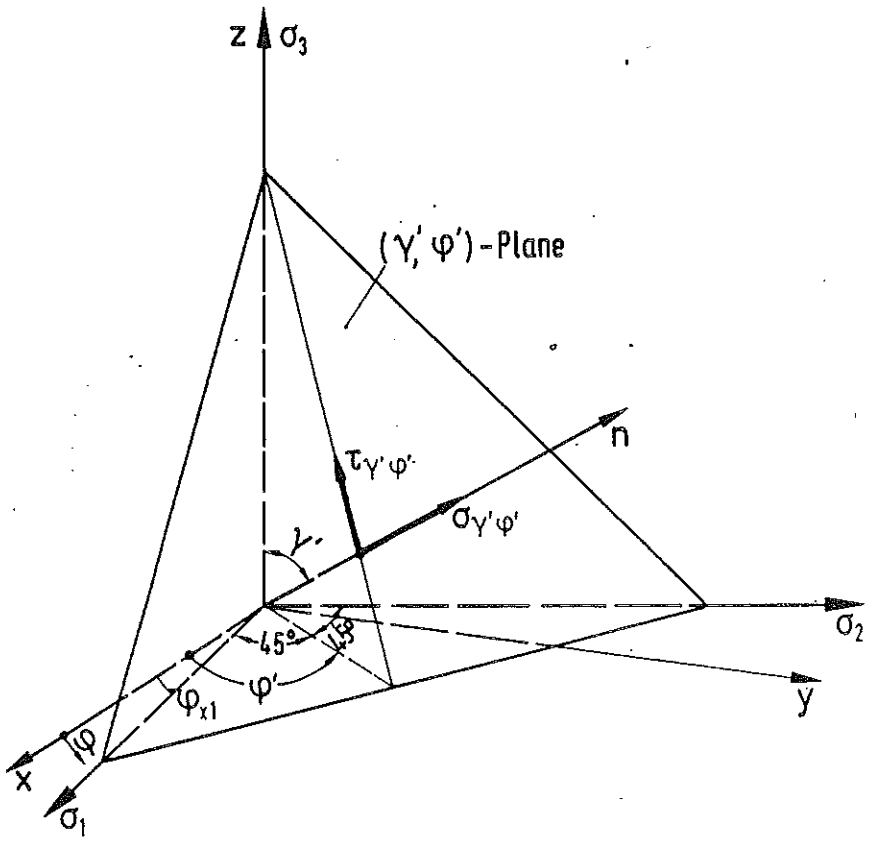

Figure 11: Position of the $(\gamma'\varphi')$–plane

2. Determination of the shear stress amplitude $\tau_{\gamma'\varphi'a}$ in the $(\gamma'\varphi')$–plane

The shear stress amplitude $\tau_{\gamma'\varphi'a}$ is taken from the stress path of the shear stress in the $(\gamma'\varphi')$– plane as half of the maximum stress range during one cycle (see Fig. 12)

$$\tau_{\gamma'\varphi'a} = \frac{1}{2}\Delta\tau_{\gamma'\varphi',max} \tag{1}$$

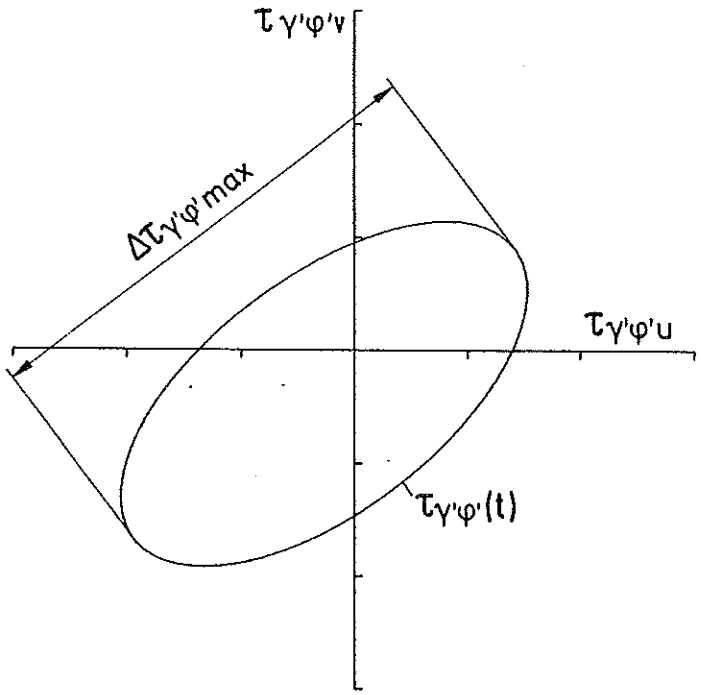

Figure 12: Stress path of shear stress $\tau_{\gamma'\varphi'}$ in $(\gamma'\varphi')$–plane

3. Determination of the material value $\tau_{\gamma'\varphi'A}$

In order to determine the value $\tau_{\gamma'\varphi'A}$ which characterizes the material response, it is assumed that in general fatigue loading the influence of the mean stress on the fatigue stress amplitude can be expressed by an equivalent mean stress σ_{meq}. It is defined as the larger one of the two stresses σ_x and σ_y, respectively, which would generate the same mean stress in the $(\gamma'\varphi')$–plane as it is caused by σ_{xm}, σ_{ym} and τ_{xym} together. From these three stress components there results a mean normal stress in the $(\gamma'\varphi')$–plane of

$$\sigma_{\gamma'\varphi'm} = \sin^2\gamma'[0.5(\sigma_{xm} + \sigma_{ym}) + 0.5(\sigma_{xm} - \sigma_{ym})\cos 2\varphi' + \tau_{xym}\sin 2\varphi'] \tag{4}$$

The equivalent mean stress for uniaxial fatigue loading is then from Eq. 4 with $\sigma_{ym} = \tau_{xym} = 0$

$$\sigma_{meq} = \frac{2\sigma_{\gamma'\varphi'm}}{\sin^2\varphi'(1+\cos 2\varphi')} \tag{5}$$

Furthermore, to determine $\tau_{\gamma'\varphi'A}$, the uniaxial fatigue stress amplitude σ_A is required. It can be calculated approximately from the alternating fatigue limit σ_W, the ultimate stress R_m and the equivalent mean stress σ_{meq} using the parabolic equation

$$\sigma_A = \sigma_W\sqrt{1-\frac{\sigma_{meq}}{R_m}} \tag{6}$$

In case of purely reversed load stresses there is $\sigma_A = \sigma_W$. The material value $\tau_{\gamma'\varphi'A}$, considered responsible for fatigue behavior and fatigue fracture, can now be calculated by the following transformation equation

$$\tau_{\gamma'\varphi'A} = 0.5\sin\varphi'\sigma_A\sqrt{\sin^2 2\varphi' + \cos^2\varphi'(1+\cos 2\varphi')^2} \tag{7}$$

5 Comparison of Test and Calculation Results

In the following the results of the experimental investigations are compared with the theoretical predictions due to the calculation method MOSH. The values to be compared are the fatigue limits of the circumferential stress amplitude σ_{uA}, and as a quality measure of the theoretical predictions the ratio

$$\frac{\sigma_{uA,test}}{\sigma_{uA,calculation}}$$

respectively the relative deviation

$$C = 1 - \frac{\sigma_{uA,test}}{\sigma_{uA,calculation}} \tag{8}$$

was taken.

		frequency ratio 1:1		frequency ratio 2:1	
Wave form	Phase difference δ	σ_{uA} $[N/mm^2]$ experimental	$\frac{\sigma_{uA}(exp.)}{\sigma_{uA}(theor.)}$	σ_{uA} $[N/mm^2]$ experimental	$\frac{\sigma_{uA}(exp.)}{\sigma_{uA}(theor.)}$
triangular	0^0	160	1.09	144	1.17
	90^0	162	1.11	141	1.04
	120^0	140	1.06		
	180^0	120	1.17		
sinusoidal	0^0	160	1.09	131	1.16
	90^0	140	1.07	139	1.10
	120^0	129	1.14		
	180^0	120	1.17		
trapezoidal	0^0	160	1.09	119	1.14
	90^0	120	1.17	126	1.16

Table 3: Comparison of test results and theoretical predictions

For the first test series concerning the influence of the wave form in combination with a phase difference on the fatigue strength—with equal frequencies of σ_{uA} and σ_{lA}—this value comes up between $C = 0.06$ and $C = 0.17$ for the entire series, as can be seen from *Table 3.* This means that the theoretical predictions result in slightly conservative deviations. The average relative deviation between theoretically and experimentally determined stress amplitudes σ_{uA} is $C = 0.125$.

There are similar results for the second test series concerning the influence of different frequencies in combination with a phase difference on the fatigue strength. Again the theoretical fatigue stress amplitudes σ_{uA} are somewhat lower than experimentally determined, as one can see from Table 3. The average relative deviation in this case is $C = 0.128$ with the theoretical results again lying on the conservative side.

6 References

[1] Nishihara, T. and Kawamoto, M.: *The strength of metals under combined alternating bending and torsion with phase difference.* Mem. of the College of Engineering, Kyoto Imperial University, Vol. XI (1945) No. 5, p. 85–112

[2] Little, R.E.: *A note on the shear stress criterion for fatigue failure under combined stress.* Aeronautical Quarterly, Vol. 20, Feb. 1969, p. 57–60

[3] Mielke, S.: *Festigkeitsverhalten metallischer Werkstoffe unter zweiachsiger schwingender Beanspruchung mit verschiedenen Spannungsverläufen.* Diss. TH Aachen, 1980

[4] Zenner, H. und Heidenreich, R.: *Festigkeitshypothese—Berechnung der Dauerfestigkeit für beliebige Beanspruchungskombinationen.* Forschungshefte FKM, Heft 55, 1976 and: *Schubspannungsintensitätshypothese—Erweiterung und experimentelle Abstützung einer neuen Festigkeitshypothese für schwingende Beanspruchung.* Forschungshefte FKM, Heft 77, 1979

[5] Issler, L.: *Festigkeitsverhalten metallischer Werkstoffe bei mehrachsiger phasenverschobener Beanspruchung.* Diss. Universität Stuttgart, 1973

[6] Simbürger, A.: *Festigkeitsverhalten zäher Werkstoffe bei einer mehrachsigen phasenverschobenen Schwingbeanspruchung mit körperfesten und veränderlichen Hauptspannungen.* LBF-Bericht Nr. FB-121, 1975

[7] Heidenreich, R., Richter, L. und Zenner, H.: *Schubspannungsintensitätshypothese—Weitere experimentelle und theoretische Untersuchungen.* Konstruktion 36, 1984, p. 99–104

[8] Nokleby, J.O.: *Fatigue under multiaxial stress conditions.* Report MD 81 001 The Norwegian Institute of Technology, Division of Machine Elements, University of Trondheim, 1981

[9] Troost, A. und El-Magd, E.: *Schwingfestigkeit bei mehrachsiger Beanspruchung ohne und mit Phasenverschiebung.* Konstruktion 33, 1981, p. 297–304

[10] Mc Diarmid, D.L.: *The effects of mean stress and stress concentration on fatigue under combined bending and twisting.* Fatigue Fracture Engineering Material Structure, Vol. 8, No. 1, 1985, p. 1–12